

Output spectrum of a detector measuring quantum oscillations

Alexander N. Korotkov

Department of Physics, State University of New York at Stony Brook, Stony Brook, NY 11794-3800

(November 1, 2018)

We consider a two-level quantum system (qubit) which is continuously measured by a detector and calculate the spectral density of the detector output. In the weakly coupled case the spectrum exhibits a moderate peak at the frequency of quantum oscillations and a Lorentzian-shape increase of the detector noise at low frequency. With increasing coupling the spectrum transforms into a single Lorentzian corresponding to random jumps between two states. We prove that the Bayesian formalism for the selective evolution of the density matrix gives the same spectrum as the conventional master equation approach, despite the significant difference in interpretation. The effects of the detector nonideality and the finite-temperature environment are also discussed.

I. INTRODUCTION

The long-standing and still controversial problem of quantum measurements¹ is gradually becoming a practical issue due to the development of experimental techniques capable of measurements at the quantum border (see, e.g. Refs.²⁻⁷). The renewed interest in this subject is caused by the needs of quantum computing,⁸ since the measurement of an entangled and possibly evolving quantum state by a realistic detector in a realistic environment presents a nontrivial problem.

Despite the experimental proof² of the violation of Bell's inequality⁹ that rejects the idea of hidden variables, the origin of the randomness of a quantum measurement result (the problem known as the "wavefunction collapse") remains controversial. Important insight into this problem has been provided by the development of the theory of continuous quantum measurement, which generalizes the "orthodox" case¹⁰ of instantaneous measurement. There are two different theoretical approaches. In the first approach¹¹ based on the theory of interaction with a dissipative environment,¹² the evolution of the density matrix of the measured system is *averaged* over a complete *ensemble* of measurements, thus leading to the deterministic equation. This is the best-known approach, at least in the solid-state community, and so can be called "conventional". The other approach¹³⁻¹⁷ (more developed in quantum optics) studies the random evolution of the quantum state during a *single* realization of the measurement, so that this evolution is conditioned on (selected by) the particular measurement result. Recently^{18,19} the latter approach has been introduced into the context of solid-state physics using the

new derivation based on the simple Bayesian analysis of probabilities.

In the present paper this Bayesian formalism is applied to the calculation of the spectral density of the detector current when a two-level quantum system (qubit) is measured continuously. As a particular example, we consider a double-quantum-dot occupied by one electron, the location of which is measured by a quantum point contact nearby.^{20,18} Another example of the setup is a single-Cooper-pair box, being measured by a single-electron transistor.^{21,19,22} One more possible example is the continuous measurement of two flux states of a SQUID by another inductively coupled SQUID.²³

We show that in the weak-coupling case when the quantum (Rabi) oscillations of the qubit state are only slightly perturbed by the detector, the corresponding peak in the spectral density of the detector current can be up to 4 times higher than the noise pedestal (see also Ref.²⁴). As the coupling increases, the Quantum Zeno effect²⁵ becomes significant leading to the Lorentzian shape of the spectral density centered at zero frequency.

It is important to notice that there should be no difference between the predictions of the conventional approach and the approach of selective evolution unless the measurement result affects the system evolution (for example, via the feedback loop). We prove this equivalence explicitly for the detector spectral density (if there is no feedback). Despite the same final result, the interpretations are different: in the Bayesian formalism a significant contribution to the spectrum comes from the correlation between the detector noise and the system evolution, while this correlation is absent in the conventional approach. In the paper we also discuss the extension of the Bayesian formalism to the case of additional weak interaction of the two-level system with a finite-temperature environment.²⁴

II. BAYESIAN FORMALISM

For a two-level quantum system described by the Hamiltonian

$$\mathcal{H}_0 = \frac{\varepsilon}{2}(c_1^\dagger c_1 - c_2^\dagger c_2) + H(c_1^\dagger c_2 + c_2^\dagger c_1) \quad (1)$$

(where ε is the energy asymmetry and H is the tunneling strength) the evolution of its density matrix ρ_{ij} due to continuous measurement is given in the conventional approach^{11,12,20,21,24} by the equations

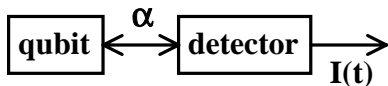


FIG. 1. Schematic of a qubit continuously measured by a detector with output signal $I(t)$.

$$\dot{\rho}_{11} = -2 \frac{H}{\hbar} \text{Im} \rho_{12}, \quad \rho_{11} + \rho_{22} = 1, \quad (2)$$

$$\dot{\rho}_{12} = \imath \frac{\varepsilon}{\hbar} \rho_{12} + \imath \frac{H}{\hbar} (\rho_{11} - \rho_{22}) - \Gamma \rho_{12}, \quad (3)$$

where the dephasing rate Γ due to measurement depends on the type of the detector used.^{5,20,21,24,26–28}

Eqs. (2)–(3) describe the averaged evolution. In contrast, to analyze the single measurement process we need the selective (conditional) evolution of ρ_{ij} which in the Bayesian formalism is described by equations¹⁸

$$\dot{\rho}_{11} = -2 \frac{H}{\hbar} \text{Im} \rho_{12} + \frac{2\Delta I}{S_0} \rho_{11} \rho_{22} [I(t) - I_0], \quad (4)$$

$$\begin{aligned} \dot{\rho}_{12} = & \imath \frac{\varepsilon}{\hbar} \rho_{12} + \imath \frac{H}{\hbar} (\rho_{11} - \rho_{22}) \\ & - \frac{\Delta I}{S_0} (\rho_{11} - \rho_{22}) [I(t) - I_0] \rho_{12} - \gamma \rho_{12}, \end{aligned} \quad (5)$$

where $I(t)$ is the detector current, $I_0 = (I_1 + I_2)/2$, I_1 and I_2 are the average currents corresponding to two localized states of the qubit, $\Delta I = I_1 - I_2$ (notice the different sign in the definition used in Ref.¹⁸), and S_0 is the low-frequency spectral density of the detector shot noise (which is assumed to be constant in the frequency range of interest and to be practically independent of the qubit state). The detector nonideality is described by the dephasing contribution $\gamma = \Gamma - (\Delta I)^2/4S_0 \geq 0$ due to interaction with “pure environment” (which does not affect the detector current). In particular, since $\Gamma = (\Delta I)^2/4S_0$ for symmetric quantum point contact (see Refs.^{20,5,24,26}), it represents an ideal detector,¹⁸ $\eta = 1$, where $\eta = 1 - \gamma/\Gamma$ is the ideality factor. In contrast, the single-electron transistor in a typical operation point is a significantly non-ideal detector, $\eta \ll 1$.^{18,21,29} (Actually, for the single-electron transistor Eq. (5) can be further improved,¹⁹ however, it does not make a difference for the purposes of the present paper.) The SQUID can be an ideal detector when its sensitivity is quantum-limited.^{30,31} Since the typical output signal from the SQUID is the voltage (not the current), this requires a minor modification of the formalism; so in this paper we do not consider the SQUID case explicitly even though all the results can be easily translated into SQUID language.

Eqs. (4)–(5) allow us to calculate the evolution of ρ_{ij} if the detector output $I(t)$ is known from the experiment. In order to simulate the measurement we need the replacement¹⁸

$$I(t) - I_0 = \Delta I (\rho_{11} - \rho_{22})/2 + \xi(t), \quad (6)$$

where the random process $\xi(t)$ has zero average and “white” spectral density $S_\xi = S_0$.

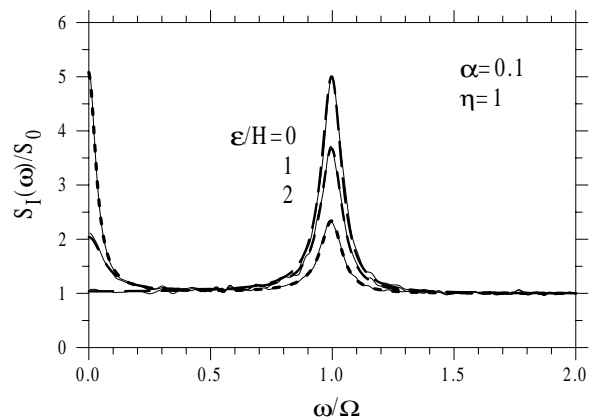


FIG. 2. Spectral density $S_I(\omega)$ of the detector current for weak coupling ($\alpha = 0.1$) of an ideal detector ($\eta = 1$) with a two-level system ($\varepsilon/H = 0, 1$, and 2). The results of the Monte-Carlo calculations using Bayesian formalism are shown by solid lines, while the dashed lines (almost coinciding with solid lines) are calculated using the master equation approach.

Notice that in order to consider the detector as a device with classical output signal, Eqs. (4)–(5) essentially use the Markov approximation and assume that the typical frequency of the internal detector evolution (on the order of $S_0/e^2 \sim I_0/e$) is much higher than the typical frequency $\max(\Omega, \Gamma)$ of ρ_{ij} evolution (here $\Omega \equiv \sqrt{4H^2 + \varepsilon^2}/\hbar$ is the frequency of unperturbed quantum oscillations). In particular, this condition requires the detector to be “weakly responding”, $|\Delta I| \ll I_0$, that allows us to use the linear response approximation.

Averaging of Eqs. (4)–(5) over all possible measurement results (i.e. over random contribution $\xi(t)$) reduces them to Eqs. (2)–(3). Notice that the stochastic equations are written in Stratonovich form which preserves the usual calculus rules, while averaging would be easier in Itô form.³²

III. WEAK COUPLING

Using Eqs. (4)–(6) and the Monte-Carlo method (similar to Ref.¹⁸) we can calculate in a straightforward way the spectral density $S_I(\omega)$ of the detector current $I(t)$. Solid lines in Fig. 2 show the results of such calculations for the ideal detector, $\eta = 1$, and weak coupling between the qubit and the detector, $\alpha = 0.1$, where $\alpha \equiv \hbar(\Delta I)^2/8S_0H$ (α is 8 times less than the parameter \mathcal{C} introduced in Ref.¹⁸). One can see that in the symmetric case, $\varepsilon = 0$, the peak at the frequency of quantum oscillations is 4 times higher than the noise pedestal, $S_I(\Omega) = 5S_0$ while the peak width is determined by the coupling strength α (see Fig. 5 below). In the asymmetric case, $\varepsilon \neq 0$, the peak height decreases (Fig. 2), while the additional Lorentzian-shape increase of $S_I(\omega)$ appears at low frequencies. The origin of this low-frequency feature

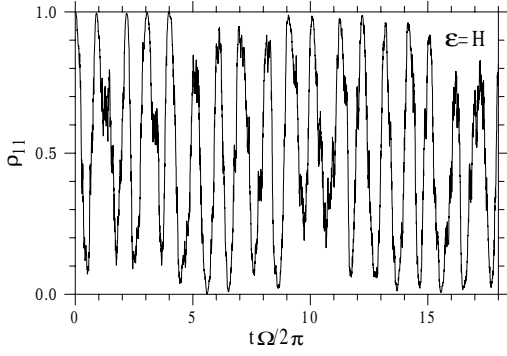


FIG. 3. A particular realization of the evolution of $\rho_{11}(t)$ due to continuous measurement for $\varepsilon/H = 1$, $\alpha = 0.1$ and $\eta = 1$. Notice the fluctuation of both the phase and the asymmetry of oscillations.

is the slow fluctuation of the asymmetry of ρ_{11} oscillations (Fig. 3). In case $\varepsilon = 0$ the amplitude of ρ_{11} oscillations is maximal (see thick line in Fig. 4a), hence there is no such asymmetry and the low-frequency feature is absent, while the spectral peak at the frequency of quantum oscillation is maximally high.

In order to understand the factor 4 for the maximum peak height, let us consider the case $\alpha \ll 1$, $\varepsilon = 0$, and $\eta = 1$. Then the selective evolution can be written as the quantum oscillations with slowly fluctuating phase $\varphi(t)$:

$$z(t) \equiv \rho_{11}(t) - \rho_{22}(t) = \cos \phi(t), \quad \phi = \Omega t + \varphi(t), \quad (7)$$

$$\rho_{12} = (i/2) \sin \phi(t) \quad (8)$$

(the state becomes pure¹⁸ after an initial transient period since $\eta = 1$, while the real part of ρ_{12} decays because of $\varepsilon = 0$). From Eqs. (4) and (6) we obtain the random phase dynamics:

$$\dot{\varphi} = -\sin \phi \frac{\Delta I}{S_0} \left[\cos \phi \frac{\Delta I}{2} + \xi(t) \right]. \quad (9)$$

Since $(\Delta I)^2/2S_0 \ll \Omega$, we can neglect the first term in the square brackets and average the second contribution over ϕ that leads to the white spectrum of $\dot{\varphi}$: $S_{\dot{\varphi}}(\omega) = (\Delta I)^2/2S_0$. Then the correlation function $K_z(\tau) \equiv \langle z(t)z(t+\tau) \rangle$ can be calculated as $K_z(\tau) = \cos(\Omega\tau) \langle \cos \Delta\varphi(\tau) \rangle / 2 = \cos(\Omega\tau) \exp[-(\Delta I)^2\tau/8S_0]/2$ and the spectral density $S_z(\omega) \equiv 2 \int_{-\infty}^{\infty} K_z(\tau) \exp(i\omega\tau) d\tau$ has a peak in the vicinity of the oscillation frequency, $|\omega - \Omega| \ll \Omega$:

$$S_z(\omega) = \frac{8S_0}{(\Delta I)^2} \frac{1}{1 + [8S_0(\omega - \Omega)/(\Delta I)^2]^2}. \quad (10)$$

The detector current is given by Eq. (6), so its spectral density consists of three contributions:

$$S_I(\omega) = S_0 + \frac{\Delta I^2}{4} S_z(\omega) + \frac{\Delta I}{2} [S_{\xi z}(\omega) + S_{z\xi}(\omega)], \quad (11)$$

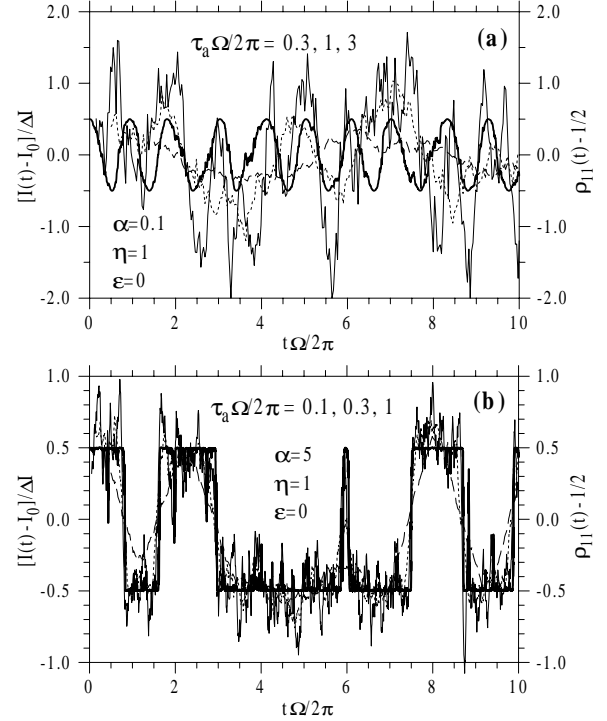


FIG. 4. A particular realization of ρ_{11} evolution (thick line) and the corresponding detector output $I(t)$ (thin solid, dotted, and dashed lines) averaged using rectangular windows with different time constants τ_a . (a) – weak coupling case, $\alpha = 0.1$, (b) – strong coupling case, $\alpha = 5$.

where the last contribution originates from the correlation between ρ_{ij} evolution and the detector noise $\xi(t)$. To calculate the correlation function $K_{\xi z}(\tau) \equiv \langle \xi(t)z(t+\tau) \rangle$ for $\tau > 0$, we need to take into account the phase shift $d\varphi = -\sin \phi \Delta I S_0^{-1} \xi(t) dt$ during even infinitesimally small time duration dt , since the amplitude of the stochastic function $\xi(t)$ grows with the timescale decrease, $\langle \xi(t)^2 dt \rangle = S_0/2$. Using trigonometric formulas and linear expansion in $d\varphi$ we obtain $\langle \xi(t) \cos[\phi(t) + d\varphi + \Omega\tau + \Delta\varphi(\tau)] \rangle = \Delta I S_0^{-1} \langle \xi(t)^2 dt \rangle \langle \sin \phi(t) \sin[\phi(t) + \Omega\tau] \rangle \langle \cos \Delta\varphi(\tau) \rangle$ and finally $K_{\xi z}(\tau) = \Delta I \cos(\Omega\tau) \exp[-(\Delta I)^2\tau/8S_0]/4$. After the Fourier transformation one finds that the correlation between $\xi(t)$ and $z(t)$ brings exactly the same contribution to the detector spectral density (see Eq. (11)) as the term due to $z(t)$ evolution, so that

$$S_I(\omega) = S_0 + \frac{4S_0}{1 + [8S_0(\omega - \Omega)/(\Delta I)^2]^2}. \quad (12)$$

Thus, the peak corresponding to quantum oscillations is 4 times higher than the noise background, while its full width at half height is equal to $(\Delta I)^2/4S_0 = \alpha\Omega$ (the same peak width has been calculated in Ref.³³). The integral under the peak,

$$\int_0^{\infty} [S(\omega) - S_0] \frac{d\omega}{2\pi} = \frac{(\Delta I)^2}{4}, \quad (13)$$

has an obvious relation to the average square of the detector current variation due to oscillations in the measured system. Notice, however, that this integral is twice as large as one would expect from the classical harmonic signal, since one half of the peak height comes from non-classical correlation between the qubit evolution and the detector noise. Classically, Eq. (13) would be easily understood if the signal was not harmonic but rectangular-like, which is obviously not the case. Actually, the detector current shows neither clear harmonic nor rectangular signal distinguishable from the intrinsic noise contribution. Figure 4a shows the simulation of ρ_{11} evolution (thick line) together with the detector current $I(t)$. Since $I(t)$ contains white noise, it necessarily requires some averaging. Thin solid, dotted, and dashed lines show the detector current averaged with different time constants τ_a : $\tau_a\Omega/2\pi = 0.3, 1,$ and $3,$ respectively. For weak averaging the signal is too noisy, while for strong averaging individual oscillation periods cannot be resolved either, so quantum oscillations can never be observed *directly* by a continuous measurement (although they can be *calculated* using Eqs. (4)–(5)). This unobservability is revealed in the relatively low peak height of the spectral density of the detector current.

IV. ARBITRARY COUPLING

The situation changes as the coupling between the detector and qubit increases, $\alpha \gtrsim 1$. The strong influence of measurement destroys quantum oscillations, and the Quantum Zeno effect²⁵ develops, so that for $\alpha \gg 1$ the qubit performs random jumps between two localized states (see Fig. 4b). In this case the properly averaged detector current follows pretty well the evolution of the qubit (however, the unsuccessful tunneling “attempts” still cannot be directly resolved), and the spectral density of $I(t)$ can be calculated using the classical theory of telegraph noise³⁴ leading to the Lorentzian shape of $S_I(\omega)$. Figure 5a shows the gradual transformation of the spectral density with the increase of the coupling α for a symmetric qubit, $\varepsilon = 0$, and an ideal detector, $\eta = 1$. The results for an asymmetric qubit, $\varepsilon/H = 1$, are shown in Fig. 5b.

The curves in Fig. 5 as well as the dashed curves in Fig. 2 are calculated using the conventional master equation approach which gives the same results for the detector spectral density as the Bayesian formalism (we will prove this later). In the conventional approach we should assume no correlation between the detector noise and the qubit evolution (the last term in Eq. (11) is absent) while the correlation function $K_{\hat{z}}(\tau)$ should be calculated considering $z(t)$ not as an ordinary function but as an operator. Then the calculation of $\langle \hat{z}(t)\hat{z}(t+\tau) \rangle$ can be essentially interpreted as follows. The first (in time) operator $\hat{z}(t)$ collapses the qubit into one of two eigenstates which correspond to localized states, then during time τ the

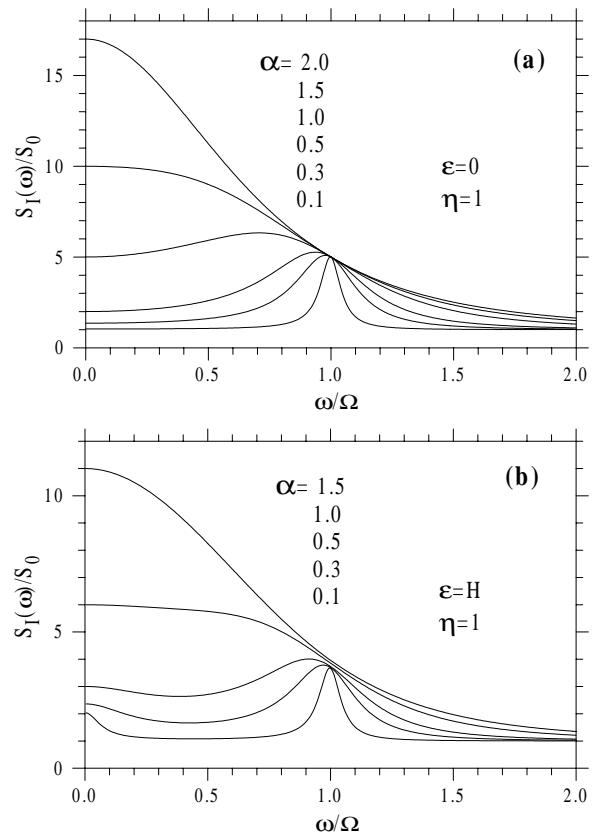


FIG. 5. The detector current spectral density $S_I(\omega)$ for $\eta = 1$ and different coupling α with (a) symmetric ($\varepsilon = 0$) and (b) asymmetric ($\varepsilon/H = 1$) qubit.

qubit performs the evolution described by conventional Eqs. (2)–(3), and finally the second operator $\hat{z}(t+\tau)$ gives the probability for the qubit to be measured in one of two localized states. (Of course, this procedure can be done purely formally,²⁴ without any interpretation.) Notice that there is complete symmetry between states “1” and “2” even for $\varepsilon \neq 0$ (in particular, in the stationary state $\rho_{11} = \rho_{22} = 1/2$), so the evolution after the first collapse can be started from any localized state leading to the same contribution to the correlation function. In this way we obviously get $K_{\hat{z}}(\tau) = \rho_{11}(\tau) - \rho_{22}(\tau)$ where ρ_{ii} is the solution of Eqs. (2)–(3) with the initial conditions $\rho_{11}(0) = 1$ and $\rho_{12}(0) = 0$.

For the symmetric qubit, $\varepsilon = 0$, these equations can be easily solved analytically, and finally we obtain:

$$S_I(\omega) = S_0 + \frac{\Omega^2(\Delta I)^2\Gamma}{(\omega^2 - \Omega^2)^2 + \Gamma^2\omega^2}, \quad (14)$$

where $\Gamma = \eta^{-1}(\Delta I)^2/4S_0 = \alpha\eta^{-1}\Omega$. This equation obviously transforms into Eq. (12) for $\eta = 1$ and $\alpha \ll 1$. Notice that for weak coupling with a nonideal detector, $\eta < 1$ and $\alpha\eta^{-1} \ll 1$, the peak height of $S_I(\omega)$ is equal to $4\eta S_0$, while the linewidth $\alpha\eta^{-1}\Omega$ of the peak is η^{-1} times wider than for the ideal detector. As the

coupling increases, the linewidth grows and the oscillation frequency decreases:³³ $\omega_{osc} = \Omega[1 - (\alpha/2\eta)^2]^{1/2}$. The transition into the overdamped regime occurs at $\alpha\eta^{-1} > 2$ while the peak-like feature disappears at $\alpha\eta^{-1} > \sqrt{2}$. For $\alpha\eta^{-1} > 2$ the spectral density consists of two Lorentzians $[\omega_{1,2} = \Gamma/2 \mp (\Gamma^2/4 - \Omega^2)^{1/2}]$ centered at zero frequency, with the negative sign and the smaller amplitude A_2 of the second Lorentzian which has higher cutoff frequency, $A_2/A_1 = -\omega_1/\omega_2$. In the case $\alpha\eta^{-1} \gg 1$, which corresponds to the well developed Quantum Zeno effect, $S_I(\omega) - S_0$ has purely Lorentzian shape $(\Delta I)^2\omega_1/(\omega^2 + \omega_1^2)$ with $\omega_1 = \Omega^2/\Gamma = \Omega\eta/\alpha$.

For the asymmetric qubit, $\varepsilon \neq 0$, the spectral density can in principle also be calculated analytically but the expressions would be too lengthy and it is simpler to use numerical solution of Eqs. (2)–(3). The analytical formula for the weak coupling limit is

$$S_I(\omega) = S_0 + \frac{\eta S_0 \varepsilon^2 / H^2}{1 + (\omega \hbar^2 \Omega^2 / 4 H^2 \Gamma)^2} + \frac{4\eta S_0 (1 + \varepsilon^2 / 2 H^2)^{-1}}{1 + [(\omega - \Omega) / \Gamma (1 - 2 H^2 / \hbar^2 \Omega^2)]^2}. \quad (15)$$

The spectral peak and the low-frequency Lorentzian become wider with the coupling increase since $\Gamma = \alpha\eta^{-1}\Omega$, and for $|\varepsilon/H| < 1/\sqrt{2}$ the overdamped regime starts from $\Gamma = \Gamma_1$ where $\Gamma_{1,2}^2 = (\Omega^2/2a)[b \mp (b^2 - 4a)^{1/2}]$, $b \equiv 1/4 - 27a^2/4 + 9a/2$, $a \equiv \varepsilon^2/(4H^2 + \varepsilon^2)$. At $\Gamma > \Gamma_2$ the dynamics formally returns to the underdamped regime, however, the peak linewidth is much larger than the frequency and so $S_I(\omega)$ is monotonous. For $|\varepsilon/H| > 1/\sqrt{2}$ the overdamped regime does not occur. In both cases in the limit of large Γ the spectral density has almost Lorentzian shape with the cutoff frequency $\omega_1 = 4H^2/\hbar^2\Gamma$.

One can check that the spectral densities given by Eqs. (14) and (15) satisfy the integral condition (13), which remains valid for arbitrary parameters α , ε/H , and η , because of the equation $K_I(+0) = (\Delta I/2)^2$.

V. EQUIVALENCE OF TWO APPROACHES

Comparing two derivations of $S_I(\omega)$ in the case $\alpha \ll 1$, $\eta = 1$, and $\varepsilon = 0$, we see that $K_{\tilde{z}}(\tau)$ is twice larger than $K_z(\tau)$ because in the conventional approach the evolution always starts from the localized state while in the Bayesian approach it starts from arbitrary phase of quantum oscillations. This difference exactly compensates for the absence of the last term in Eq. (11) in the conventional approach.

Let us prove explicitly that the two approaches give the same result for $S_I(\omega)$ in a general case. In order to calculate $K_{\xi z}(\tau)$ for $\tau > 0$ using the Bayesian formalism, let us first average the product $\xi(t_0)z(t_0 + \tau)$ over random $\xi(t)$ during time period $t_0 < t < t_0 + \tau$, fixing the same conditions at $t = t_0$. Then we can use conventional Eqs.

(2)–(3) [regarded as Eqs. (4)–(6) averaged over random $\xi(t)$] with the initial condition $\rho_{ij}(t_0 + 0) = \rho_{ij}(t_0) + d\rho_{ij}$ where

$$dz = \Delta I S_0^{-1} [1 - z^2(t_0)] \xi(t_0) dt, \quad (16)$$

$$d\rho_{12} = -\Delta I S_0^{-1} z(t_0) \rho_{12}(t_0) \xi(t_0) dt \quad (17)$$

(for simplicity we will refer to $z \equiv \rho_{11} - \rho_{22}$ as a component of ρ_{ij}). Since the sign of $\xi(t_0)$ is arbitrary and averaged evolution equations are linear, we need only the fluctuating contribution to $\rho_{ij}(t_0 + 0)$ and, hence, can formally assume that the evolution starts from $\rho_{ij}(t_0 + 0) = d\rho_{ij}$ (notice that we can forget the condition $\rho_{11} + \rho_{22} = 1$ and use only z and ρ_{12}). Using the relation $\xi(t_0)^2 dt = S_0/2$ and the evolution linearity, we can formally write

$$K_{\xi z}(\tau) = (\Delta I/2) \langle \tilde{z}(t_0 + \tau) \rangle, \quad (18)$$

where $\tilde{\rho}_{ij}$ satisfies Eqs. (2)–(3) with $\tilde{z}(t_0) = 1 - z(t_0)^2$ and $\tilde{\rho}_{12}(t_0) = -z(t_0)\rho_{12}(t_0)$, and the averaging over the initial conditions at $t = t_0$ should still be done later. Before that let us do a similar formal trick for $K_z(\tau)$ representing it as $\langle \tilde{z}(t_0 + \tau) \rangle$ where the evolution starts from $\tilde{z}(t_0) = z(t_0)^2$ and $\tilde{\rho}_{12}(t_0) = z(t_0)\rho_{12}(t_0)$. Now combining two terms in the detector current correlation function $K_I(\tau) \equiv \langle I(t_0)I(t_0 + \tau) \rangle - \langle I \rangle^2 = (\Delta I/2)^2 K_z(\tau) + (\Delta I/2) K_{\xi z}(\tau)$ (here $\tau > 0$), we see that it can be written as $(\Delta I/2)^2 \langle \tilde{z}(t_0 + \tau) \rangle$ where $\tilde{z}(t_0) = 1$ and $\tilde{\rho}_{12}(t_0) = 0$. Thus we have exactly arrived at the expression of the conventional approach, in which the evolution always starts from the localized state, regardless of the actual quantum state at $t = t_0$. This proof is obviously valid for arbitrary α , η , and ε/H . Despite the same result in two approaches, the interpretations are quite different since the Bayesian approach allows us to follow the qubit evolution during the measurement process, while the conventional approach gives only the average characteristics.

VI. FINITE-TEMPERATURE ENVIRONMENT

In this section we will discuss how to introduce the finite-temperature environment into Eqs. (4)–(6) of the Bayesian formalism. Notice that so far there has been complete symmetry between the states “1” and “2” even for finite energy difference ε , while the finite temperature effects would be expected to lead to different average populations of these states. Such symmetry requires an implicit assumption that the typical energy in the detector (voltage or temperature) is much larger than the energies involved in the qubit dynamics. So, the absence of temperature in the formalism does not mean that it is zero or very large, it just means that the temperature effects are not important. Now let us assume that besides the detector, the qubit is coupled to an additional finite-temperature environment, which creates an asymmetry between states “1” and “2” when $\varepsilon \neq 0$.

While the case of finite coupling of a two-level system with an environment presents a really difficult problem,¹² the weak coupling limit can be treated in a simple way. In the standard method³⁵ it is described by the equations

$$\dot{\rho}_{++} = -\gamma_1(\rho_{++} - p_{st}), \quad \rho_{++} + \rho_{--} = 1, \quad (19)$$

$$\dot{\rho}_{+-} = i\Omega\rho_{+-} - \gamma_2\rho_{+-}, \quad (20)$$

which are written in the diagonal basis (“+” corresponds to the ground state). The temperature T determines the stationary occupation $p_{st} = [1 + \exp(-\hbar\Omega/T)]^{-1}$ of the ground state, and the relaxation rates obey inequality³⁵ $\gamma_1/2 \leq \gamma_2 \ll \Omega$.

If the coupling of the qubit with the detector is also weak, $\alpha\eta^{-1} \ll 1$, the evolution due to extra finite-temperature environment can be simply added to the evolution due to measurement. For this purpose Eqs. (19)–(20) should be translated into the basis of localized states, so the terms

$$-(A^2\gamma_1 + B^2\gamma_2)(\rho_{11} - 1/2) - \gamma_1 A(1/2 - p_{st}) + AB(\gamma_1 - \gamma_2) \text{Re}\rho_{12}, \quad (21)$$

$$\text{where } A \equiv \varepsilon/\hbar\Omega, \quad B \equiv 2H/\hbar\Omega,$$

should be added into Eq. (4) for $\dot{\rho}_{11}$ and the terms

$$-(A^2\gamma_2 + B^2\gamma_1) \text{Re}\rho_{12} + AB(\rho_{11} - \rho_{22})(\gamma_1 - \gamma_2)/2 + \gamma_1 B(1/2 - p_{st}) - i\gamma_2 \text{Im}\rho_{12} \quad (22)$$

should be added into Eq. (5) for $\dot{\rho}_{12}$. The same terms should obviously be added into Eqs. (2)–(3) for the conventional approach. (Of course, this generalization is purely phenomenological and is limited to the weak coupling regime, so the effect of Eqs. (21)–(22) can be considered only at the timescale longer than oscillation period.)

In the generalized case it is still possible to prove that the results of the Bayesian formalism for the detector current spectral density $S_I(\omega)$ exactly coincide with the results of the conventional approach. The essential difference from the proof above is nonzero stationary solution $(z_{st}, \rho_{12,st})$ of modified Eqs. (2)–(3) when $p_{st} \neq 1/2$. It is convenient to consider homogeneous evolution equations (with $p_{st} = 1/2$) simply shifting $z(t)$ and $\rho_{12}(t)$ by the stationary values. Using the same idea as in the proof above we can show that in the Bayesian approach $K_I(\tau)$ for $\tau > 0$ can be written as $(\Delta I/2)^2 \langle \tilde{z}(t_0 + \tau) \rangle$ where $\tilde{\rho}_{ij}$ satisfies homogeneous modified Eqs. (2)–(3) with $\tilde{z}(t_0) = 1 - 2z_{st}z(t_0) + z_{st}^2$ and $\tilde{\rho}_{12}(t_0) = -z(t_0)\rho_{12,st} - z_{st}\rho_{12}(t_0) + z_{st}\rho_{12,st}$. After the averaging over initial states these initial conditions can be replaced with $\tilde{z}(t_0) = 1 - z_{st}^2$ and $\tilde{\rho}_{12}(t_0) = -z_{st}\rho_{12,st}$.

Now let us show that we get the same $K_I(\tau)$ in the conventional approach. With the probability $(1 + z_{st})/2$ the first operator $\hat{z}(t_0)$ localizes the qubit into the state “1”. Then the initial state for the homogeneous equations is $\tilde{z}(t_0) = 1 - z_{st}$, $\tilde{\rho}_{12}(t_0) = -\rho_{12,st}$. With the probability $(1 - z_{st})/2$ the evolution starts from the state “2”, i.e. $\tilde{z}(t_0) = -1 - z_{st}$, $\tilde{\rho}_{12}(t_0) = -\rho_{12,st}$. Adding two

contributions with opposite signs we see again that for $\tau > 0$, $K_I(\tau) = (\Delta I/2)^2 \tilde{z}(t_0 + \tau)$ where \tilde{z} can be found as a solution of Eqs. (2)–(3) modified by Eqs. (21)–(22) without inhomogeneous terms, with the initial condition $\tilde{z}(t_0) = 1 - z_{st}^2$ and $\tilde{\rho}_{12}(t_0) = -z_{st}\rho_{12,st}$. Thus, the correlation function $K_I(\tau)$ and, hence, the spectral density $S_I(\omega)$ coincide in the two approaches.

It is technically simpler to consider the averaged evolution in the diagonal basis rather than in the basis of localized states [for this purpose we need to translate the term $-\Gamma\rho_{12}$ from Eq. (3) into the diagonal basis and add it into Eqs. (19)–(20)]. So, to calculate the correlation function $K_{\tilde{z}}(\tau)$ analytically, we start the evolution from one of the localized states, then consider the averaged evolution in the diagonal basis (neglecting the rapidly oscillating terms due to measurement), and make the second projection onto localized states at $t = \tau$. Finally we obtain the result²⁴

$$S_I(\omega) = S_0 + \frac{(\Delta I)^2}{W_t} \left[\frac{\varepsilon^2}{\hbar^2\Omega^2} - z_{st}^2 \right] \frac{1}{1 + (w/W_t)^2} + \frac{2(\Delta I)^2 H^2}{W_0 \hbar^2 \Omega^2} \frac{1}{1 + [(\omega - \Omega)/W_0]^2} \quad (23)$$

where

$$z_{st} = \frac{\varepsilon}{\hbar\Omega} \frac{1}{1 + 4H^2\Gamma/\gamma_1\hbar^2\Omega^2} \tanh\left(\frac{\hbar\Omega}{2T}\right), \quad (24)$$

$$W_t = \gamma_1 + \frac{4\Gamma H^2}{\hbar^2\Omega^2}, \quad (25)$$

$$W_0 = \gamma_2 + \frac{\Gamma}{2} \left(1 + \frac{\varepsilon^2}{\hbar^2\Omega^2}\right). \quad (26)$$

Let us emphasize that the effect of finite-temperature environment is not generally equivalent to the nonideality of the detector described by finite γ in Eq. (5). As an example, in the case of extra environment the right hand part of Eq. (13) should be multiplied by the factor $1 - z_{st}^2$ which disappears ($z_{st} = 0$) only if $T = \infty$ or $\varepsilon = 0$.

Comparing Eqs. (23) and (15) one can see that within the accuracy of weak coupling approximation the change of $S_I(\omega)$ due to extra environment can be reduced to the detector nonideality, $\eta < 1$, in two cases. If $|\varepsilon/H| \ll 1$, then Eqs. (23) and (15) coincide at arbitrary temperature T for $\eta = (1 + 2\gamma_2/\alpha\Omega)^{-1}$. For asymmetric qubit, $|\varepsilon/H| \gtrsim 1$, the equivalence is possible only at high temperatures, $T \gg \hbar\Omega$, and requires conditions

$$\gamma_2 = \gamma_1(1 + \varepsilon^2/2H^2)/2, \quad (27)$$

$$\eta^{-1} = 1 + (1 + \varepsilon^2/4H^2)^{3/2}\gamma_1/\alpha\Omega. \quad (28)$$

Figure 6 shows the numerically calculated spectral density $S_I(\omega)$ of the detector current for a nonideal detector, $\eta = 0.5$ (dashed lines) and for an ideal detector but extra coupling of the qubit to the environment at temperature $T = H$ (solid lines). The rates γ_1 and γ_2 are chosen according to Eqs. (27) and (28). For the symmetric qubit, $\varepsilon = 0$, the results of two models practically coincide. In

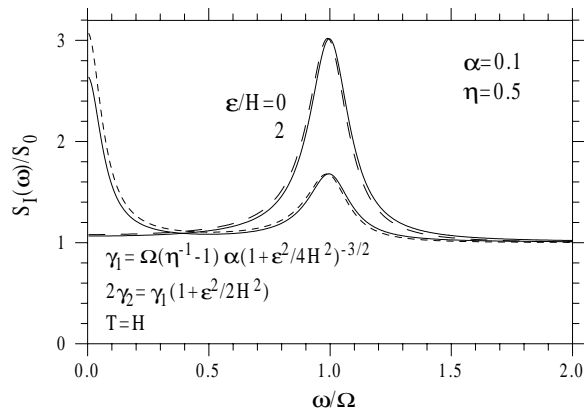


FIG. 6. Spectral density $S_I(\omega)$ for the nonideal detector (dashed lines) and for the case of the ideal detector and weak extra coupling with the finite-temperature environment, $T = H$ (solid lines).

contrast, the solid and dashed lines for $\varepsilon = 2H$ significantly differ from each other at low frequencies, while the spectral peak at $\omega \sim \Omega$ is fitted quite well.

VII. CONCLUSION

Using both Bayesian and conventional approaches, we have calculated the spectral density $S_I(\omega)$ of the detector current when a two-level quantum system (qubit) is measured continuously. Depending on the coupling strength, there is a gradual transition from quantum oscillations to quantum jumps. This results in a transition from the peak-like spectral density to the Lorentzian shape of $S_I(\omega)$. The maximal height of the peak at the frequency of quantum oscillation is shown to be 4 times the shot noise pedestal (see also Ref.²⁴).

In the simple case of weak coupling between a symmetric qubit and an ideal detector, the height of the spectral peak is twice as high as the classical result for a harmonic signal. In the Bayesian approach this is explained by the significant correlation between the detector noise and the further evolution of the measured system due to quantum back-action. In contrast, in the conventional approach this fact is the consequence of discrete eigenvalues of \hat{z} operator, which corresponds to the magnitude measured by the detector. (In other words, this operator “collapses” the system into one of two eigenstates, and that is why the averaged product of two operators is twice as large as that for a classical harmonic signal.) So, even though the results for $S_I(\omega)$ coincide in two approaches, the interpretations are significantly different since the “abrupt” collapse is replaced in the Bayesian approach by the “continuous” collapse related to the noisy detector output.

It is important to notice that the Bayesian formalism allows us to monitor continuously the *phase* of quantum

oscillations. This makes it possible to tune the phase using the feedback control of the qubit parameters. If the real-time calculations using Eqs. (4)–(5) and fast feedback loop were available in an experiment (the typical bandwidth should be larger than Γ) then the random diffusion of the oscillation phase could be eliminated and the qubit could “stay fresh” for a very long time. The suppression of qubit dephasing using the feedback control of the tunneling strength H has been confirmed by the Monte-Carlo simulations. The elimination of the phase diffusion gives rise to the δ -function peak in the detector spectral density $S_I(\omega)$ at the frequency Ω . A detailed analysis of this situation is beyond the scope of the present paper.

The author thanks D. V. Averin, J. E. Lukens, and K. K. Likharev for fruitful discussions. The work was partly supported by AFOSR.

- ¹ *Quantum Theory of Measurement*, ed. by J. A. Wheeler and W. H. Zurek (Princeton Univ. Press, 1983).
- ² A. Aspect, J. Dalibar, and G. Roger, *Phys. Rev. Lett.* **49**, 1804 (1982).
- ³ W. M. Itano, D. J. Heinzen, J. J. Bollinger, and D. J. Wineland, *Phys. Rev. A* **41**, 2295 (1990).
- ⁴ V. B. Braginsky and F. Ya. Khalili, *Quantum measurement* (Cambridge Univ. Press, 1992).
- ⁵ E. Buks, R. Schuster, M. Heiblum, D. Mahalu, and V. Umansky, *Nature* **391**, 871 (1998).
- ⁶ Y. Nakamura, Yu. A. Pashkin, and J. S. Tsai, *Nature* **398**, 786 (1999).
- ⁷ D. Sprinzak, E. Buks, M. Heiblum, and H. Shtrikman, *cond-mat/9907162*.
- ⁸ C. Bennett, *Phys. Today*, Oct. 1995, 24 (1995).
- ⁹ J. S. Bell, *Physics* **1**, 195 (1964).
- ¹⁰ J. von Neumann, *Mathematical Foundations of Quantum Mechanics* (Princeton Univ. Press, Princeton, 1955).
- ¹¹ W. H. Zurek, *Phys. Today*, **44** (10), 36 (1991).
- ¹² A. O. Caldeira and A. J. Leggett, *Ann. Phys. (N.Y.)* **149**, 374 (1983).
- ¹³ N. Gisin, *Phys. Rev. Lett.* **52**, 1657 (1984).
- ¹⁴ H. J. Carmichael, *An open system approach to quantum optics*, Lecture notes in physics (Springer, Berlin, 1993).
- ¹⁵ M. J. Gagen, H. M. Wiseman, and G. J. Milburn, *Phys. Rev. A* **48**, 132 (1993).
- ¹⁶ M. B. Plenio and P. L. Knight, *Rev. Mod. Phys.* **70**, 101 (1998).
- ¹⁷ M. B. Mensky, *Phys. Usp.* **41**, 923 (1998).
- ¹⁸ A. N. Korotkov, *Phys. Rev. B* **60**, 5737 (1999); *quant-ph/9808026*.
- ¹⁹ A. N. Korotkov, in *Proceedings of LT'22* (Helsinki, 1999) and *cond-mat/9906439*.
- ²⁰ S. A. Gurvitz, *Phys. Rev. B* **56**, 15215 (1997); *quant-ph/9808058*.
- ²¹ A. Shnirman and G. Schön, *Phys. Rev. B* **57**, 15400 (1998).

- ²² Y. Makhlin, G. Schön, and A. Shnirman, cond-mat/0001423.
- ²³ S. Han, J. Lapointe, and J. E. Lukens, Phys. Rev. Lett. **66**, 810 (1991).
- ²⁴ A. N. Korotkov and D. A. Averin, cond-mat/0002203.
- ²⁵ B. Misra and E. C. G. Sudarshan, J. Math. Phys. **18**, 756 (1977).
- ²⁶ I. L. Aleiner, N. S. Wingreen, and Y. Meir, Phys. Rev. Lett. **79**, 3740 (1997).
- ²⁷ Y. Levinson, Europhys. Lett. **39**, 299 (1997).
- ²⁸ L. Stodolsky, Phys. Lett. B **459**, 193 (1999).
- ²⁹ From the corrected Eqs. (34) and (37) of Ref.²¹ in weakly responding case ($|\Delta I| \ll I_0$), the “measurement rate” is $(\Delta I)^2/4S_0 = dE^2(\Gamma_R^2/R_L - \Gamma_L^2/R_R)^2[8e^4\Gamma_L\Gamma_R(\Gamma_L + \Gamma_R)(\Gamma_L^2 + \Gamma_R^2)]^{-1}$, while the dephasing rate is $\Gamma = dE^2\Gamma_L\Gamma_R/\hbar^2(\Gamma_L + \Gamma_R)^3$, that gives the ideality factor $\eta = \hbar^2(\Gamma_R^2/R_L - \Gamma_L^2/R_R)^2(\Gamma_L + \Gamma_R)^2[8e^4\Gamma_L^2\Gamma_R^2(\Gamma_L^2 + \Gamma_R^2)]^{-1}$, where Γ_L and Γ_R are the tunneling rates through two junctions of single-electron transistor, $R_{L,R} \gg \hbar/e^2$ are their tunnel resistances, and dE is the energy coupling with the measured system. In the case $\Gamma_L \sim \Gamma_R$ we have significantly nonideal detector, $\eta \ll 1$; however, for $\Gamma_L \ll \Gamma_R$ one obtains $\eta = (\hbar/e^2 R_L)^2(\Gamma_R/\Gamma_L)^2/8$ that becomes comparable to unity when $\Gamma_L/\Gamma_R \lesssim \hbar/e^2 R_L$, i.e. when the cotunneling contribution becomes important.
- ³⁰ V. V. Danilov, K. K. Likharev, and A. B. Zorin, IEEE Trans. Magn. MAG-**19**, 572 (1983).
- ³¹ D. V. Averin, *International symposium on mesoscopic superconductivity* (Atsugi, Japan, 2000), Abstracts, p. 89.
- ³² B. Øksendal, *Stochastic differential equations* (Springer, Berlin, 1992).
- ³³ G. Hackenbroich, B. Rosenow, and H. A. Weidenmüller, Phys. Rev. Lett. **81**, 5896 (1998).
- ³⁴ S. Machlup, J. Appl. Phys. **25**, 341 (1954).
- ³⁵ U. Weiss, *Quantum dissipative systems* (World Scientific, Singapore, 1993).